



Size effects in plasma-enhanced nano-transfer adhesion

Journal:	<i>Soft Matter</i>
Manuscript ID	SM-ART-09-2018-001862.R1
Article Type:	Paper
Date Submitted by the Author:	12-Oct-2018
Complete List of Authors:	Deagen, Michael; Rensselaer Polytechnic Institute, Materials Science and Engineering Chan, Edwin; NIST, Polymer Division Schadler, Linda; Rensselaer Polytechnic Institute, Materials Science and Engineering Ullal, Chaitanya; Rensselaer Polytechnic Institute, Materials Science and Engineering

Cite this: DOI: 10.1039/xxxxxxxxxx

Size effects in plasma-enhanced nano-transfer adhesion[†]

Michael E. Deagen,^{a,b} Edwin P. Chan,^c Linda S. Schadler,^{a,b} and Chaitanya K. Ullal^{a,b*}Received Date
Accepted Date

DOI: 10.1039/xxxxxxxxxx

www.rsc.org/journalname

Plasma bonding and layer-by-layer transfer molding have co-existed for decades, and here we offer a combination of the two that drives both techniques to the nanoscale. Using fluorinated elastomeric stamps, lines of plasma-treated poly(dimethylsiloxane) (PDMS) were stacked into multi-layer woodpile structures via transfer molding, and we observe a pronounced size effect wherein nanoscale lines (≤ 280 nm period) require ultra-low plasma dose (< 20 J) and fail to bond at the much higher range of plasma dose (600 J to 900 J) recommended in the PDMS plasma bonding literature. The size effect appears to be related to the thickness of the oxide film that develops on the PDMS surface during treatment, and we employ an empirical relationship, $h_{ox} \approx 0.25 \times \sqrt{dose}$, to estimate the thickness of this film in the low plasma dose (< 100 J) regime. The empirical relationship shows good agreement with existing studies on plasma-treated PDMS oxide film thickness, and the transition between successful transfer and delamination coincides well with a critical value of the oxide thickness relative to the thickness of the transferred layer. Through peel testing, we identified a transition in failure mode of flat plasma-bonded PDMS consistent with the optimal plasma dose in previous literature but otherwise observed strong, irreversible adhesion even at ultra-low plasma dose. By demonstrating the importance of low plasma dose for plasma-enhanced nano-transfer adhesion, these results advance our understanding of irreversible adhesion of soft materials at the nanoscale and open up new opportunities within the relatively unstudied ultra-low dose plasma treatment regime.

1 Introduction

The ability to rapidly print three-dimensional micro- and nano-structures in an additive, layer-by-layer fashion at low cost has transformative potential in the fields of photonics, microfluidics and mechanical metamaterials.^{1–4} Transfer molding, in which an elastomeric stamp with micro- or nanoscale relief structures is filled with an ink material, placed against a substrate, and peeled away to reveal the transferred pattern, has shown promise by enabling multi-layer fabrication in a defect-tolerant and massively parallel approach.^{5,6} To avoid capillary wicking of the ink into unwanted areas of the substrate, the ink is sometimes partially cured prior to the transfer step. By fully curing the ink and using a thin, wetting polymer film as an adhesive layer, the transfer molding process was extended to the micron scale.⁷

To improve the adhesion of polymers such as poly(dimethylsiloxane) (PDMS), surface treatment through exposure to plasma has been widely implemented and studied for several decades.^{8–10} Oxidation at the PDMS surface upon exposure to plasma introduces hydrophilic (-OH) groups that undergo a condensation reaction when placed in contact with another hydrophilic surface (e.g., glass, oxidized PDMS) to form a strong, irreversible bond.^{11,12} Continued exposure to plasma forms a densely crosslinked, silica-like film.^{10,13} The extent of plasma oxidation is impacted by several process variables including plasma power, process gas, chamber pressure, and duration of exposure. Recently, the extent of oxidation at the surface was found to be well-characterized by a dose parameter ($power \times duration$).^{14,15} While not all PDMS bonding studies report both plasma power and duration, those that do typically report an optimal plasma dose equivalent to a range of 600 J to 900 J.^{16–20}

Here, we implement plasma treatment of PDMS lines within perfluoropolyether (PFPE) stamps for multi-layer transfer molding at the micro- and nanoscale and observe a size effect wherein successful nanoscale transfer necessitates ultra-low plasma doses (< 20 J) and fails at higher doses through brittle delamination of

^a Department of Materials Science and Engineering, Rensselaer Polytechnic Institute, Troy, NY 12180, USA; E-mail: ullalc@rpi.edu

^b Center for Lighting Enabled Systems and Applications, Rensselaer Polytechnic Institute, Troy, NY 12180, USA

^c Materials Science and Engineering Division, National Institute of Standards and Technology, Gaithersburg, MD 20899, USA.

[†] Electronic Supplementary Information (ESI) available: Onset of delamination of PDMS lines. See DOI: 10.1039/cXsm00000x/

the pattern upon removal of the stamp (Figure 1). The size effect reveals brittle failure at plasma doses orders of magnitude before macroscopically brittle behavior such as surface cracking would be expected.^{10,21} PFPE serves as a useful stamp material for its low surface energy, ideal wetting properties for residual-free filling of PDMS ink, and inability to form strong interfacial bonds following plasma treatment.^{22,23}

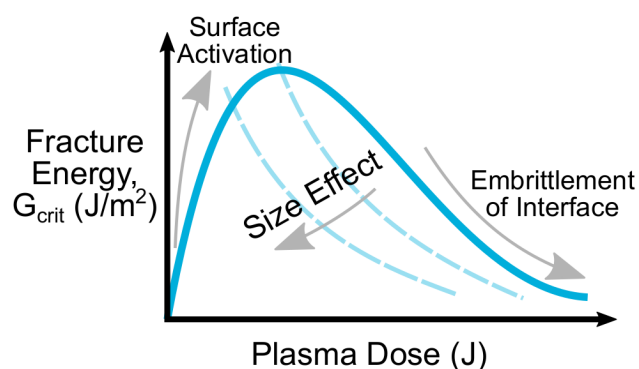


Fig. 1 Expected adhesion of plasma-bonded PDMS as a function of plasma dose (solid curve), with dashed lines representing the size effect of nano-transfer adhesion at progressively smaller scales.

A review of studies that quantify oxide thickness of plasma-treated PDMS is presented in terms of plasma dose and found to have good agreement across the varying experimental approaches to measure oxide thickness.^{15,24,25} We find that these data are captured by a simple empirical relationship, $h_{ox} \approx 0.25 \times \sqrt{\text{dose}}$, that supports the observed size effect phenomenon for plasma doses below 100 J. Peel tests of flat plasma-bonded PDMS showed maximum peel force coinciding with the optimal plasma dose suggested by the literature, however the quantitative interpretation of this maximum may be influenced by the transition in failure mode from interfacial to cohesive failure. Meanwhile, strong, irreversible bonding was achieved even at ultra-low plasma dose. These results add a new dimension to the existing plasma bonding literature, enable transfer molding at smaller size scales, and open up new possible avenues of research in ultra-low plasma doses for plasma-enhanced nano-transfer adhesion.

2 Methods

2.1 Materials

Silicon master patterns with rectangular grooves, spaced at a 50 % duty cycle with aspect ratio (h/w) of approximately 0.6, were purchased from LightSmyth Technologies (Eugene, OR) with pattern periods of 139 nm, 278 nm, 600 nm, and 6 μm and groove depths of 50 nm, 110 nm, 190 nm, and 1.7 μm , respectively. Perfluoropolyether (PFPE) stamps were made with Fluorolink MD-700 from Cornerstone Technology (Newark, DE) combined with 1 mass% 2,2-dimethoxy-2-phenylacetophenone (DMPA) photoinitiator from Sigma Aldrich. Low-viscosity PDMS ink for filling stamps was prepared by mixing vinyl-terminated PDMS of 6,000 g/mol weight average molecular mass (DMS-V21), 5 mass % vinyl modulator (SIT7900.0), and 17 mass % (25 to 35 % methylhydrosiloxane)dimethylsiloxane copolymer (HMS-

301) from Gelest (Morrisville, PA). 500 mg/L Pt (II) acetylacetonate (Sigma Aldrich) was used as a catalyst. For peel tests, Sylgard 184 PDMS from Dow Corning (Midland, MI) was prepared in a 10:1 ratio of base to crosslinker by mass.

2.2 Stamp and Ink Preparation

PFPE pre-polymer was inserted between a flat backplane of Sylgard 184 PDMS (UV-transparent) and the silicon master pattern to make stamps sufficiently thin to provide good conformal contact with a substrate, and cured under 365 nm Ultraviolet (UV) light (UV-A 6-watt Hand Lamp, VWR) in an atmosphere of N_2 . Stamps were filled by selectively dewetting PDMS ink into the grooves of the stamp²² and using a stream of N_2 to remove residual droplets. Ink was cured inside the stamp by exposing to 365 nm UV light for 15 min followed by at least 1 hr in an oven at 110 $^\circ\text{C}$.

2.3 Plasma Treatment

Air plasma treatment was performed in a PDC-32G plasma cleaner from Harrick Plasma (Ithaca, NY) at 107 Pa [800 mTorr] using a power of 18 W unless otherwise stated. Duration of plasma exposure was controlled manually with the aid of a digital timer. Both stamp and substrate were placed simultaneously in the chamber for plasma treatment. Following treatment, the chamber was immediately vented and the stamp was placed in contact with the substrate within 1 min. Stamp and substrate were held under mild pressure in a clamp assembly (≈ 15 N applied force) to ensure conformal contact between the stamp and substrate.

2.4 Peel Testing

Flat peel samples of Sylgard 184 PDMS with 10 mm width and approximately 0.5 mm thickness were prepared by casting in molds and degassing in a vacuum desiccator prior to thermally curing at 110 $^\circ\text{C}$ for 30 min. Following plasma treatment, a piece of Kapton tape was placed at the end of one sample to prevent irreversible bonding in the grip region for the peel tester. Samples were brought into conformal contact within 1 min of plasma treatment and left for several hours prior to peel testing.

Peel tests were performed on a TA-XT2i Texture Analyser from Stable Micro Systems (Surrey, United Kingdom) with a 5 kg load cell and fixed crosshead velocity of 0.5 mm/s. Peel tests were performed in a T-Peel configuration where the peel angle is 180 $^\circ$ and the critical energy release rate, G_{crit} , for a sample of given width, w , according to the Kaelble equation²⁶ simplifies to

$$G_{crit} = \frac{2F}{w}. \quad (1)$$

Peel force, F , was calculated by averaging across the steady-state peel force plateau. In the event of cohesive failure, where the measured peel force reached a peak and sudden drop-off, the average force near failure was taken.

3 Results

3.1 Size Dependence of Transfer Success

A randomized full factorial experiment comparing the effects of feature size and plasma exposure shows the range of treatments that result in successful transfer for various feature sizes (Figure 2). Successful transfer refers to fracture at the stamp-ink interface, while delamination involves partial or complete fracture at the ink-substrate interface during demolding, or peeling, of the stamp. The substrate in each case was a single layer of PDMS lines of the same feature size well-bonded on glass, which were exposed to the same plasma treatment conditions as the ink being transferred. Control experiments, where no plasma treatment was performed, showed complete delamination. An important aspect of this plot is that, at the normally suggested plasma bonding dose of 600 J to 900 J from the previous literature (approximately 30 s to 45 s at 18 W), only the largest pattern exhibits successful transfer. Additionally, an ultra-low plasma dose (18 J) showed successful transfer for all feature periods except 140 nm. 600 nm patterns at 10 s plasma duration and 280 nm patterns at 3 s duration showed an intermediate region between successful transfer and complete delamination (see Supplementary Figure S1).

3.2 Estimating Oxide Thickness

The thickness of the oxide film that forms on plasma-treated PDMS has been quantified by others through TEM cross-sections (Béfahy *et al.*),²⁴ X-ray reflectometry (Bayley *et al.*),¹⁵ and AFM nano-indentation (Sarrazin *et al.*).²⁵ Bayley *et al.* plotted oxide thickness as a function of plasma dose and modeled the kinetics of oxide formation as a frontal propagation following a logarithmic dependence that accelerates between film formation and film propagation stages. The others reported oxide thickness as a function of plasma duration, which can then be converted to dose by incorporating the reported power values. While these studies implemented different measurement techniques, the combined data show good agreement (Figure 3). We find that these data roughly follow a simple parabolic relationship, $h_{ox} \approx 0.25 \times \sqrt{dose}$, reminiscent of diffusion-controlled thermal oxidation of silicon at longer times.²⁷ Thermal oxidation of silicon actually follows a linear dependence at short times, however a parabolic relationship nonetheless provides a useful estimate of the oxide thickness for plasma-treated PDMS in the low-dose (<100 J) regime.

3.3 Critical Oxide Thickness for Transfer

We use the empirical, parabolic relationship from Figure 3 in the low and ultra-low (<100 J) plasma dose regime to estimate the oxide thickness, h_{ox} , as a function of the total thickness, d_0 , of the transferred layer. Plotting the normalized oxide thickness and identifying points corresponding to experimentally observed transfer or delamination from Figure 2 shows a clear transition where, once the oxide thickness surpasses approximately 1.5 % of the total thickness of the features being transferred, the pattern undergoes brittle delamination from the substrate upon peeling of the stamp (Figure 4). The results suggest that, even at low plasma dose, the silica-like oxidized layer becomes detrimental

to transfer when nanoscale PDMS lines are plasma-bonded in a multi-layer woodpile configuration.

Follow-on experiments were performed at lower and higher plasma doses on 140 nm and 6 μm patterns, respectively, to probe the limits of transfer molding through plasma treatment (Figure 5). Expected plasma dose leading to the onset of delamination for the 140 nm and 6 μm patterns are 9.0 J and 10 kJ, respectively. Low-dose treatments on 140 nm patterns were performed at 7 W for 0.5 s and 1 s (3.5 J and 7 J), and high-dose treatments on 6- μm patterns were performed at 18 W for 1.5 min, 3 min, and 10 min (1.6 kJ, 3.2 kJ, and 10.8 kJ).

At the lowest plasma dose of 3.5 J, lines with a period of 140 nm demonstrated improved transfer compared to 7 J and above. However, collapse and coalescence of the lines indicates that, upon removal of the stamp, some delamination occurred. Lines with a period of 6 μm treated at higher plasma doses showed an onset of delamination at around 1.6 kJ dose and a greater extent of delamination at 3.2 kJ, while the sample exposed to 10.8 kJ showed complete delamination upon removal from the stamp. The fracture surfaces of 6 μm lines following delamination appear to become more brittle at higher plasma dose, with the highest dose showing diminished evidence of conformal contact between the layers (see Supplementary Figure S2).

3.4 Peel Testing of Flat PDMS

To investigate the optimal PDMS bonding parameters (600 J to 900 J) typically found in the literature, peel tests were performed. This range corresponds to approximately 30 s to 45 s plasma exposure at 18 W. Adhesion between flat slabs of PDMS was quantified through the critical energy release rate, G_{crit} , for crack propagation. Control samples (no plasma treatment) separated with negligible force, below the resolution of the equipment. At relatively low plasma dose, samples failed through steady-state crack propagation at the interface between the bonded samples. Samples treated at higher plasma dose failed in a cohesive manner by tearing through the bulk of the PDMS sample instead of maintaining separation at the original bonded interface (Figure 6). The cohesive fracture energy of PDMS is 100 J/m² to 400 J/m².²⁸

3.5 Transfer Molding Beyond Two Layers

Applying the knowledge of low-dose plasma treatments that favor successful transfer molding at the sub-micron scale, 4- and 6-layer woodpile structures of PDMS with a period of 600 nm were patterned in a layer-by-layer manner onto glass substrates (Figure 7). Each layer was patterned by simply rotating the stamp 90° for each additional layer without precise registration to the substrate. Both PDMS-filled PFPE stamp and the substrate were placed simultaneously in the plasma chamber for 3 s at 18 W. The stamp was placed onto the substrate within 1 min after plasma exposure and held under moderate pressure for at least two hours at room temperature prior to stamp removal.

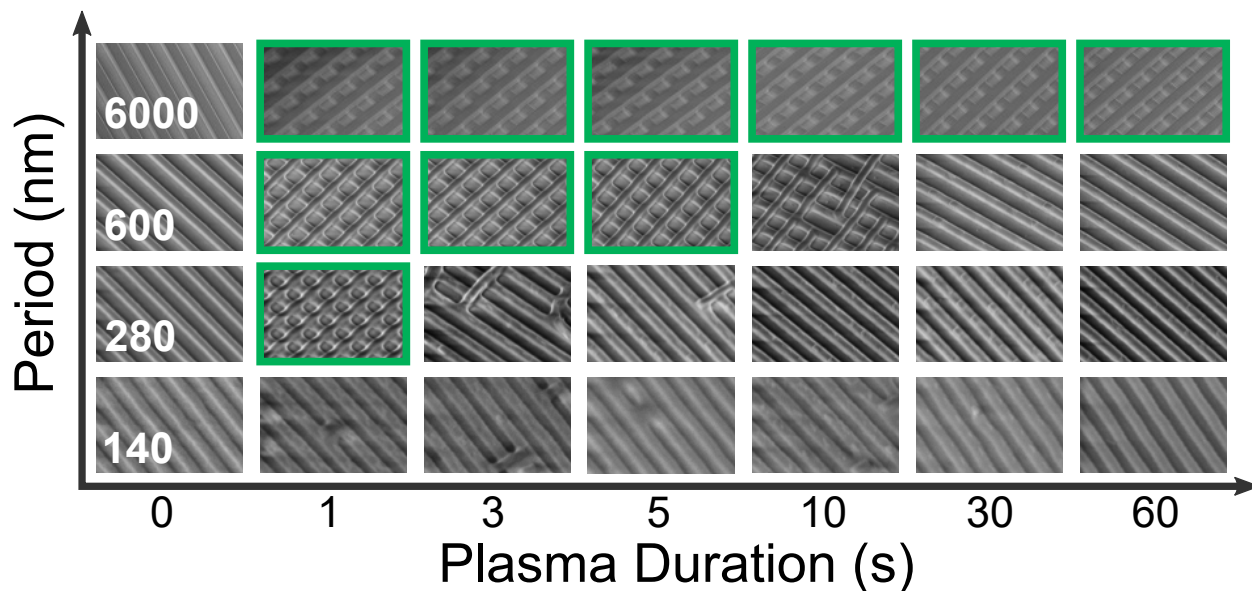


Fig. 2 Size dependence on transfer success as a function of plasma duration at 18 W power, with conditions showing successful transfer outlined in green.

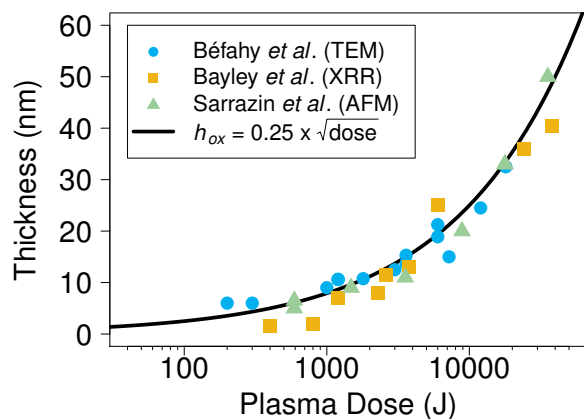


Fig. 3 Review of the literature quantifying oxide film thickness of plasma-treated PDMS, plotted in terms of thickness vs. plasma dose. The solid black line shows an empirical, parabolic relationship between oxide thickness and dose that fits the data well within this regime.

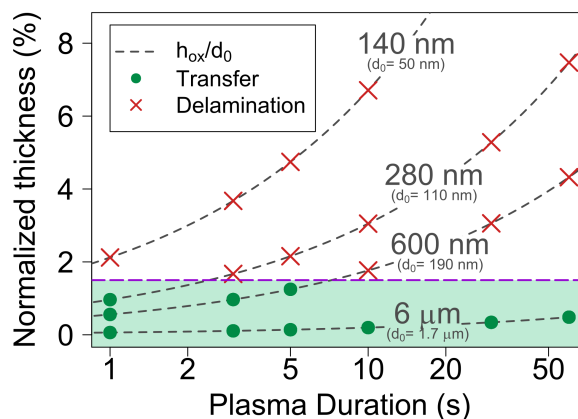


Fig. 4 Correlating experimentally observed regions of transfer and delamination for various feature periods to the normalized expected thickness of the oxide film. Dashed curves represent the expected thickness of the oxide, h_{ox} , relative to the thickness of the layer being transferred, d_0 , based on the parabolic approximation $h_{ox} \approx 0.25 \times \sqrt{dose}$. A horizontal dashed line is drawn at 1.5%. Plasma treatment was performed at 18 W.

4 Discussion

4.1 Lower and Upper Limits to Plasma Dose

At vanishingly low plasma doses, adhesion is limited by surface coverage of hydrophilic groups that provide covalent bonding sites at the interface. Ye *et al.* studied the conversion of PDMS surfaces exposed to plasma and found that the methyl concentration decreases exponentially with first order kinetics and a time constant of 0.3 min (27 Pa [200 mTorr], 18 W).²⁹ Our results at ultra-low plasma dose show that the surface functionalization occurs more rapidly than at the times typically used for bonding. Activation of the surface occurs even for our shortest practical exposure times as evidenced by the strong, irreversible bonding shown in peel tests for these ultra-low plasma doses. Separately,

we observe partial delamination of 140 nm period lines below the expected transition of 9 J; the continued improvement in transfer from 7 J to 3.5 J implies that the delamination is still a result of the oxide film as opposed to a lack of surface coverage of hydrophilic groups.

At high plasma dose, we observe an earlier onset of delamination of 6- μm period lines (1.6 kJ) than would be expected if the observed size effect due to h_{ox}/d_0 continued to scale (10 kJ). This onset of brittle delamination is consistent with the brittle separation observed for flat PDMS treated at high plasma doses.^{21,24} As both the thickness, h , and Young's modulus, E , of the oxidized PDMS surface increase upon continued plasma exposure,

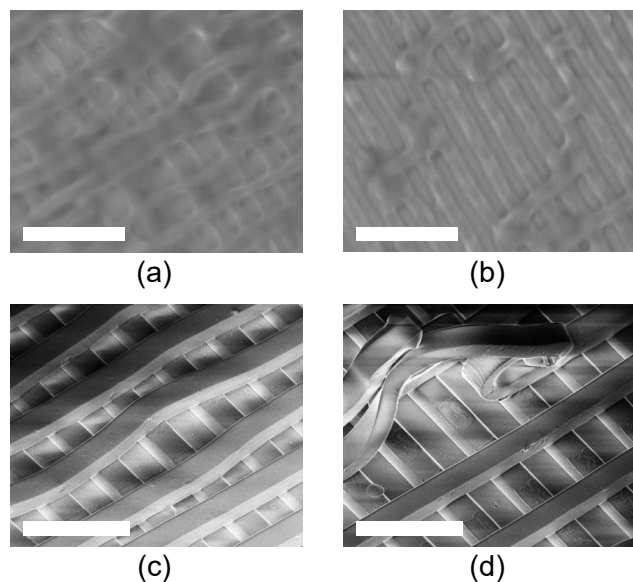


Fig. 5 Top-down SEM images of 140 nm period lines at plasma treatment doses of (a) 3.5 J and (b) 7 J. Tilted SEM images of 6 μm period lines at plasma doses of (c) 1.6 kJ and (d) 3.2 kJ. Scale bars are 500 nm (a, b) and 10 μm (c, d).

the flexural rigidity, a function of Eh^3 , diminishes the compliance of the PDMS to the substrate and subsequently reduces the effective contact area for covalent bonding at the interface. A crack propagating along this brittle interface would encounter less resistance due to the reduced effective contact area and overall reduced interfacial toughness. Adhesion enhancement of flat PDMS at intermediate plasma doses (600 J to 900 J) coincides with crack propagation into the bulk material through cohesive failure. Conventional wisdom would state that the transition to cohesive failure occurs when the interfacial bond energy exceeds the cohesive fracture energy of the bulk material. Our peel test results on flat PDMS show that an ultra-low plasma dose provides an immediate increase in adhesion sufficient for transfer, with adhesion eventually decreasing at much higher plasma doses, consistent with the existing literature.^{16,17,20} In the case of patterned PDMS however the growth of the oxide film offsets any further increase in surface functionalization by preventing successful transfer of sub-micron structures at intermediate plasma doses.

4.2 Size Dependence of Plasma-Enhanced Nano-Transfer Adhesion

During peeling, demolding stresses exerted by the stamp favor delamination unless the ink-substrate interfacial bond is sufficiently robust for successful transfer. On a structured substrate (e.g., woodpile structure), ink-substrate contact area is diminished while demolding stress becomes concentrated at edges along the bonded interface. Flat PDMS exhibits strong, irreversible bonding from ultra-low to intermediate doses, however we find that only ultra-low plasma doses favor transfer of nanoscale lines (≤ 280 nm period). These results do not necessarily imply complete saturation of hydrophilic groups on the PDMS surface at ultra-low doses, but rather point to a size effect that emerges during trans-

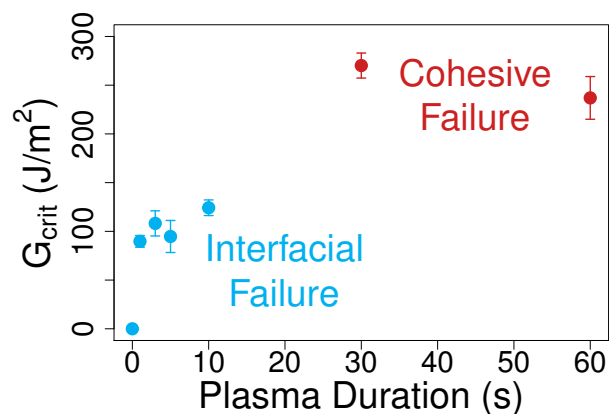


Fig. 6 Peel test measurements of the critical energy release rate, G_{crit} , for flat PDMS as a function of plasma duration with plasma power of 18 W. Error bars represent standard deviation for the three replicates tested under each condition. Samples treated at a low plasma dose separated at the interface, while those treated at the two highest plasma doses all failed cohesively.

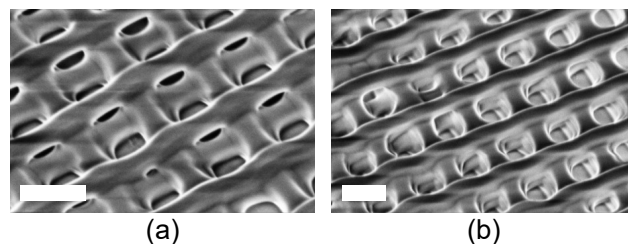


Fig. 7 Woodpile structures comprising (a) 4 and (b) 6 layers of PDMS lines with 600 nm period, patterned layer-by-layer using low-dose plasma treatments of 54 J (18 W, 3 s). Scale bars are 500 nm.

fer molding at the nanoscale. Based on the expected oxide film thickness for a given plasma treatment dose, we see a rapid transition toward delamination when the oxide film surpasses about 1.5 % of the thickness of the transferred layer.

This experimentally observed trend favors the idea that, below a certain feature size, the thickness of the oxidized PDMS surface layer no longer becomes negligible in the context of interfacial adhesion. Considering the intensity of the stress field at the crack tip during peeling,³⁰ delamination is expected to occur when the peak stress at the crack tip exceeds the fracture strength of the interface. Large features, by blunting the crack tip, effectively distribute demolding stresses such that the size effect is not observed and delamination occurs at the much higher plasma doses consistent with flat plasma-bonded PDMS. On the other hand, small features may locally magnify the demolding stress, sensitizing the pattern to interfacial failure once the oxide reaches a critical thickness. The critical value is expected to depend on various other factors that affect local peel mechanics at the interface such as pattern shape, aspect ratio, inclination angle of stamp sidewalls, and relative area of contact with the substrate.

Factors that affect the growth of the oxide film itself include pressure, concentration of O_2 , and treatment type. At higher

plasma treatment pressure, where ions in the plasma have a shorter mean free path and higher frequency of collisions with the surface, improved adhesion is expected due to rapid functionalization of the surface while minimizing the rate of oxide propagation into the bulk. Given the relatively unexplored regime of low and ultra-low plasma treatment dose, more research and development in techniques and tools for achieving such low doses would aid in the continued progress of plasma-enhanced nano-transfer adhesion.

4.3 Nano-Transfer Molding of Soft Ink Materials

PDMS serves as a useful model material for studying multi-layer transfer molding due to its favorable wetting properties as an ink and capability of adhesion enhancement through plasma treatment. At the micro-scale, PDMS maintains its mechanical integrity in a woodpile configuration. At the sub-micron scale, we observe sagging of woodpile structure likely due to a combination of increased surface area and reduced energy to deform the structure leading to the tendency of the lines to collapse. The energetic balance between reduction in free surface and bending of the structure is similarly observed through buckling and collapse of PDMS structures with high aspect ratio.³¹ To reduce the amount of deformation of the structure, one could reduce the applied pressure to maintain conformal contact of the stamp with the substrate, or use a stiffer PDMS formulation as the ink material such as h-PDMS.³² Nonetheless, given the bio-compatible nature of PDMS, the collapsed structures may still be of interest for the study of biological cell interactions with tailored micro- and nano-structures. Addition of inorganic fillers into the ink material could also add interesting properties and enable various other functionalities.³³ Through implementation of ultra-low dose plasma treatment for nano-scale adhesion, researchers may continue to advance benchtop prototyping capabilities of multi-layer nanoscale materials and devices.

5 Conclusions

Transfer molding through plasma treatment was implemented at the sub-micron scale for multi-layer patterning of PDMS lines, demonstrating a size effect that favors low and ultra-low plasma doses for successful transfer. Using an empirical relationship to estimate the thickness of the surface oxide film at low plasma doses, $h_{ox} \approx 0.25 \times \sqrt{dose}$, we find that a transition between successful transfer and delamination occurs once the oxide film reaches a critical value approximately 1.5 % of the layer thickness. Peel tests of flat plasma-bonded PDMS showed an immediate increase in adhesion upon ultra-low plasma dose (<20 J) and an eventual transition to cohesive failure at approximately 600 J, consistent with the range of optimal dose in the PDMS plasma bonding literature (600 J to 900 J). Lower and upper limits to plasma bonding outside the size effect range appear to be the surface coverage of hydrophilic groups and embrittlement of the interface, respectively. Applying low plasma dose to multi-layer transfer molding of PDMS lines led to 4- and 6-layer woodpile structures. These results improve upon the understanding of PDMS plasma-bonding at the nanoscale, highlight the benefits of

ultra-low plasma dose, and push the field of multi-layer transfer molding to newer, smaller size scales.

6 Conflicts of Interest

There are no conflicts to declare.

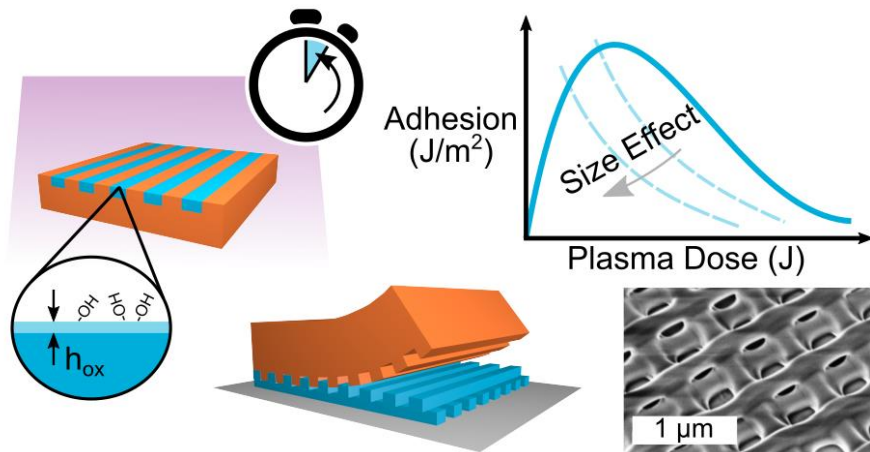
7 Acknowledgements

This article is based on work supported by the National Science Foundation under cooperative agreement EEC-0812056, the Graduate Research Fellowship Program under Grant No. DGE-1247271, and New York State under NYSTAR contract C090145. Any opinion, findings, and conclusions or recommendations expressed in this article are those of the authors and do not necessarily reflect the views of the National Science Foundation. Certain instruments and materials are identified in this paper to adequately specify the experimental details. Such identification does not imply recommendation by the National Institute of Standards and Technology; nor does it imply that the materials are necessarily the best available for the purpose. This work is a contribution of NIST, an agency of the U.S. Government, and not subject to U.S. copyright. The authors would like to extend gratitude to Prof. Catalin Picu, Dr. Christopher M. Stafford, Aditya Prasad, and Marissa Giovino for helpful conversations.

References

- 1 J.-H. Lee, P. Kuang, W. Leung, Y.-S. Kim, J.-M. Park, H. Kang, K. Constant and K.-M. Ho, *Appl. Phys. Lett.*, 2010, **96**, 94.
- 2 M. R. Beaulieu, N. R. Hendricks and J. J. Watkins, *ACS Photonics*, 2014, **1**, 799–805.
- 3 M. A. Unger, H.-P. Chou, T. Thorsen, A. Scherer and S. R. Quake, *Science*, 2000, **288**, 113–116.
- 4 J.-H. Lee, J. P. Singer and E. L. Thomas, *Adv. Mater.*, 2012, **24**, 4782–4810.
- 5 X.-M. Zhao, Y. Xia and G. M. Whitesides, *Adv. Mater.*, 1996, **8**, 837–840.
- 6 X.-M. Zhao, Y. Xia and G. M. Whitesides, *J. Mater. Chem.*, 1997, **7**, 1069–1074.
- 7 J.-H. Lee, C.-H. Kim, K.-M. Ho and K. Constant, *Adv. Mater.*, 2005, **17**, 2481–2485.
- 8 L. J. Gerenser, *J. Adhes. Sci. Technol.*, 1993, **7**, 1019–1040.
- 9 G. S. Ferguson, M. K. Chaudhury, H. A. Biebuyck and G. M. Whitesides, *Macromolecules*, 1993, **26**, 5870–5875.
- 10 M. J. Owen and P. J. Smith, *J. Adhes. Sci. Technol.*, 1994, **8**, 1063–1075.
- 11 M. K. Chaudhury and G. M. Whitesides, *Langmuir*, 1991, **7**, 1013–1025.
- 12 D. C. Duffy, J. C. McDonald, O. J. A. Schueller and G. M. Whitesides, *Anal. Chem.*, 1998, **70**, 4974–4984.
- 13 H. Hillborg, J. F. Ankner, U. W. Gedde, G. D. Smith, H. K. Yasuda and K. Wikström, *Polymer*, 2000, **41**, 6851–6863.
- 14 A. Chiche, C. M. Stafford and J. T. Cabral, *Soft Matter*, 2008, **4**, 2360–2364.
- 15 F. A. Bayley, J. L. Liao, P. N. Stavrinou, A. Chiche and J. T. Cabral, *Soft Matter*, 2014, **10**, 1155–1166.

- 16 B.-H. Jo, L. M. Van Lerberghe, K. M. Motsegood and D. J. Beebe, *J. Microelectromech. S.*, 2000, **9**, 76–81.
- 17 S. Bhattacharya, A. Datta, J. M. Berg and S. Gangopadhyay, *J. Microelectromech. S.*, 2005, **14**, 590–597.
- 18 M. A. Eddings, M. A. Johnson and B. K. Gale, *J. Micromech. Microeng.*, 2008, **18**, 067001.
- 19 S. H. Kim, Y. Cui, M. J. Lee, S.-W. Nam, D. Oh, S. H. Kang, Y. S. Kim and S. Park, *Lab Chip*, 2011, **11**, 348–353.
- 20 C.-f. Chen and K. Wharton, *RSC Adv.*, 2017, **7**, 1286–1289.
- 21 K. L. Mills, X. Zhu, S. Takayama and M. D. Thouless, *J. Mater. Res.*, 2008, **23**, 37–48.
- 22 M. E. Deagen, L. S. Schadler and C. K. Ullal, *ACS Appl. Mater. Inter.*, 2017, **9**, 36385–36391.
- 23 S. G. Im, K. W. Bong, C.-H. Lee, P. S. Doyle and K. K. Gleason, *Lab Chip*, 2009, **9**, 411–416.
- 24 S. B efahy, P. Lipnik, T. Pardo en, C. Nascimento, B. Patris, P. Bertrand and S. Yunus, *Langmuir*, 2009, **26**, 3372–3375.
- 25 B. Sarrazin, R. Brossard, P. Guenoun and F. Malloggi, *Soft Matter*, 2016, **12**, 2200–2207.
- 26 D. H. Kaelble, *T. Soc. Rheol.*, 1960, **4**, 45–73.
- 27 B. E. Deal and A. S. Grove, *J. Appl. Phys.*, 1965, **36**, 3770–3778.
- 28 C.-f. Chen, *J. Adhes. Sci. Technol.*, 2018, **32**, 1239–1252.
- 29 H. Ye, Z. Gu and D. H. Gracias, *Langmuir*, 2006, **22**, 1863–1868.
- 30 A. Crocombe and R. Adams, *J. Adhesion*, 1981, **12**, 127–139.
- 31 E. Delamarche, H. Schmid, B. Michel and H. Biebuyck, *Adv. Mater.*, 1997, **9**, 741–746.
- 32 H. Schmid and B. Michel, *Macromolecules*, 2000, **33**, 3042–3049.
- 33 H. Goesmann and C. Feldmann, *Angew. Chem. Int. Edit.*, 2010, **49**, 1362–1395.



Multi-layer transfer molding of plasma-bonded PDMS lines at the nanoscale was achieved through ultra-low dose plasma treatment.